TISSUE ENGINEERING: Part C
Volume 16, Number 6, 2010

DOI: 10.1089/ten.tec.2009.0776

Cancellous Bone Osseointegration Is Enhanced by *In Vivo* Loading

Bettina M. Willie, Ph.D.,[1,*] Xu Yang, M.D.,[1] Natalie H. Kelly, B.S.,[1] Jane Han, B.S.,[1] Turya Nair, B.S.,[1] Timothy M. Wright, Ph.D.,[1] Marjolein C.H. van der Meulen, Ph.D.,[1,2] and Mathias P.G. Bostrom, M.D.[1]

Biophysical stimuli may be an effective therapy to counteract age-related changes in bone structure that affect the primary stability of implants used in joint replacement or fracture fixation. The influence of controlled mechanical loading on osseointegration was investigated using an *in vivo* device implanted in the distal lateral femur of 12 male rabbits. Compressive loads (1 MPa, 1 Hz, 50 cycles/day, 4 weeks) were applied to a porous titanium foam implant and the underlying cancellous bone. The contralateral limbs served as nonloaded controls. Backscattered electron imaging indicated that the amount of bone ingrowth was significantly greater in the loaded limb than in the nonloaded control limb, whereas the amount of underlying cancellous periprosthetic bone was similar. No significant difference in the mineral apposition rate of the bone ingrowth or periprosthetic bone was measured in the loaded compared to the control limb. Histological analysis demonstrated newly formed woven bone in direct apposition to the implant coating, with a lack of fibrous tissue at the implant–periprosthetic bone interface in both loaded and nonloaded implants. The lack of fibrous tissue demonstrates that mechanical stimulation using this model significantly enhanced cancellous bone ingrowth without the detrimental effects of micromotion. These results suggest that biophysical therapy should be further investigated to augment current treatments to enhance long-term fixation of orthopedic devices. Additionally, this novel *in vivo* loading model can be used to further investigate the influence of biophysical stimulation on other tissue engineering approaches requiring bone ingrowth into both metallic and nonmetallic cell-seeded scaffolds.

Introduction

Osseointegration, a structural connection between bone and an implant surface[1] to achieve cementless fixation, has been successfully achieved in many orthopedic device applications.[2–11] However, cementless fixation outcomes have been suboptimal in cases of compromised femoral or tibial bone for total hip and knee arthroplasty, respectively, and in revision surgery. To improve outcomes, bone ingrowth research has focused on improving porous metallic implant materials.[12–14] Little attention has been paid toward finding ways to enhance the underlying cancellous bone tissue with which the implants interact. A promising strategy to enhance bone ingrowth is the harnessing of the adaptive response of bone to controlled mechanical loading.

In several experimental models, cortical bone osseointegration has been enhanced by mechanical loading,[15–17] which has implications in hip replacement. However, the more clinically relevant concern in the context of joint replacement and fracture fixation is the adaptive response of cancellous bone. The paucity of available experimental models has been a limitation in studying the adaptive response of cancellous bone to mechanical loading.[18,19] For osseointegration studies, mechanical loading must be conducted to avoid excessive micromotion at the bone–implant interface, which could impede bone ingrowth. Bone chamber models have been used; however, these models measure *de novo* bone formation or tissue differentiation rather than adaptation of preexisting bone to mechanical loading[20–25] and are extremely sensitive to the chosen micromotion parameters.[25]

Relative motion between the implant and cancellous bone should not exceed about 150 μm, above which fibrous tissue rather than bone ingrowth dominates.[26,27] Bone ingrowth can still occur in implants subjected to 150 μm of motion, but the bone ingrowth is separated from the periprosthetic host bone by an encapsulating layer of fibrous tissue at the interface between the porous coating and the periprosthetic host bone.[28] Similarly, a weight-bearing canine model of a porous coated device implanted in cancellous bone of the distal femur[27] demonstrated that controlled movements in the range of 500 μm relative to the surrounding bone resulted

[1]Hospital for Special Surgery, New York, New York.
[2]Sibley School of Mechanical and Aerospace Engineering, Cornell University, Ithaca, New York.
*Present address: Julius Wolff Institut, Charité-Universitätsmedizin Berlin, Berlin, Germany.

in fibrous tissue formation, but with subsequent immobilization the fibrous tissue reverted to bone.[29]

The current investigation examined the influence of controlled mechanical loading on cancellous bone osseointegration into a porous titanium foam implant, using an *in vivo* device implanted in the distal lateral femur of a rabbit. The porous titanium foam implant has previously demonstrated robust osteoconductive properties, resulting in a comparable bone ingrowth to that of conventional sintered beaded implants in a distal femur rabbit model.[30] Previously, our research group developed and used this model to study native cancellous bone adaptation *in situ* without a porous titanium foam implant.[18,31] These studies directly loaded the cancellous host bone using the implantable loading device. We demonstrated that the number of loading cycles and loading duration modulated the cancellous response. Trabecular bone volume fraction increased and trabeculae thickened to reduce the strains experienced in the bone tissue with loading and stiffen the tissue in the loading direction.[31] In the current study, the model was adapted to incorporate a porous implant placed between the cancellous host bone and the loading device to test the hypothesis that cancellous bone osseointegration would be enhanced in the loaded limb compared to the nonloaded contralateral control limb.

Materials and Methods

Experimental model and loading regime

After Institutional Animal Care and Use Committee approval, a porous implant and a loading device were implanted bilaterally into the lateral surface of the distal femur of 12 skeletally mature (31 weeks old) male New Zealand white rabbits. Two rabbits were euthanized immediately after bilateral implantation to provide time zero baseline data. In the remaining 10 rabbits, the right femur was subjected to compressive loads. The contralateral left femur served as a control, with the device surgically implanted, but without subsequent loading. The implantation of bilateral loading chambers and porous implant required 60 min of surgical anesthesia (induced with a cocktail of 0.05 mg/kg atrophine sulfate, 35 mg/kg ketamine hydrochloride, and 0.5 mg/kg acetylpromazine injected intramuscularly and maintained by isoflurane inhalation). The operative procedure was performed aseptically, and antibiotic prophylaxis was administered (25 mg/kg ampicillin). Analgesia was administered postoperatively (0.05 mg/kg buprenorphine).

A standard posterior lateral surgical approach was used to expose the condyle.[18] A guide was used to remove the cortical bone with a custom routing device (4.5 mm diameter) to a depth of 1 mm, using constant irrigation to minimize heat necrosis. The milling guide was removed, and the stationary baseplate portion of the *in vivo* loading device was secured to the cortex of the lateral femoral condyle via two bicortical screws. Once the baseplate was securely attached, the porous implant was placed inside the stationary baseplate in direct contact with the cancellous bone. The top of the loading device was set to the locked position by turning the top piece in a clockwise direction, preventing the loading core from sliding within the base and inadvertently applying a load to the porous implant (Fig. 1). The wounds were thoroughly irrigated, and the skin closed in layers over the top piece of the loading device with resorbable chromic sutures followed by interrupted surgical sutures. The external wounds were treated with a local antiseptic solution.

The cylindrical, 5-mm-diameter, 2-mm-long porous implants (Smith and Nephew, Inc., Memphis, TN) were monoblocks of porous titanium foam with a cell diameter of $\sim$900 μm, an interconnecting pore diameter of $\sim$300 μm (mean void intercept length of 565.1 ± 170.6 μm), and an average porosity of 74.4%. Mean void intercept length and porosity measurements were determined by 2D metallography techniques. The implants were packaged and gamma sterilized (25–45 kGy).

Beginning 1 day after surgery, the top of the implanted loading device was manually unlocked and compressive loads (1 MPa, 1 Hz, 50 cycles/day) were applied daily for 4 weeks through the skin to the top surface of the implanted device in the right femur of each rabbit. The loading core of the implanted loading device was allowed to slide within its base, applying a sinusoidal compressive load to the surface of the porous titanium foam implant. Loads were applied using an automated system (Fig. 1) that implemented an electromagnetic actuator to deliver direct, controlled compressive loads to the top of the loading device. The actuator (BEI Kimco LA24-20-000A, San Marcos, CA) was controlled by the voltage output from a function generator (AFG320; Tektronix, Beaverton, OR) interfaced with an amplifier (Kepco BOP 21-10M, Flushing, NY). A load cell (Model 31, 25 lb; Sensotec Honeywell, Columbus, OH) was positioned in line with the actuator for load calibration and data collection. The loading parameters used have been shown in previous studies[18,31] to lead to increased trabecular bone volume fraction, trabecular

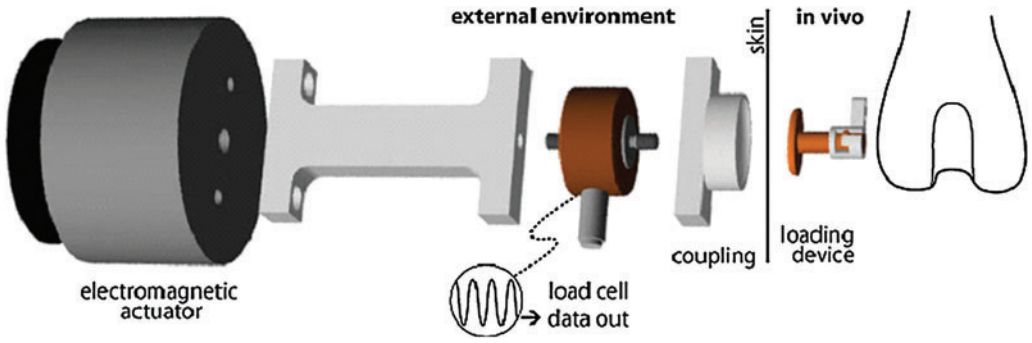

FIG. 1. Schematic of load train from actuator to cancellous bone. Color images available online at www.liebertonline.com/ten.

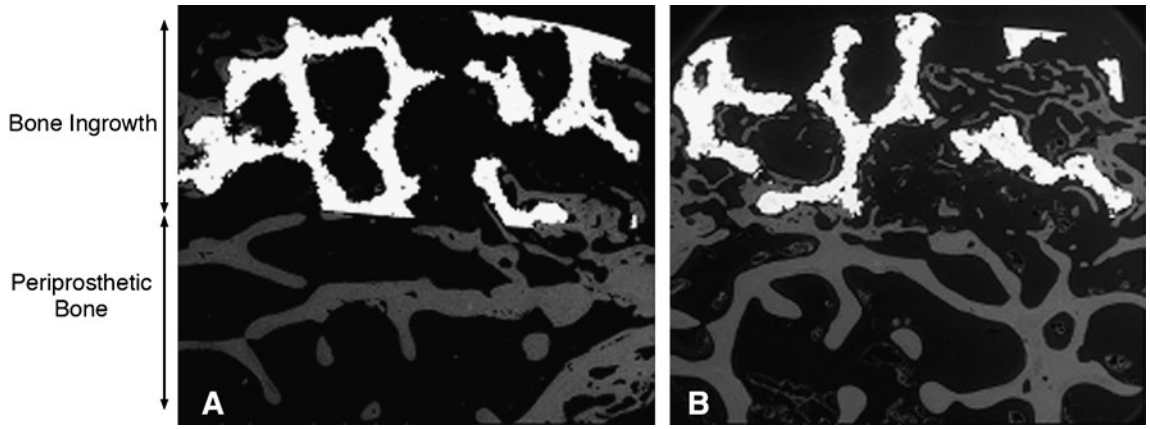

FIG. 2. Backscattered electron images (50×) comparing the control limb (**A**) to the loaded contralateral limb (**B**) from the same rabbit. Bone ingrowth (gray) can be observed within the porous titanium implant (white). The regions analyzed for bone ingrowth and periprosthetic bone are shown with two-headed arrows.

thickness, mean intercept length, and mineral apposition rate (MAR) relative to the contralateral control limbs. After loading, the implanted loading device was manually locked again to limit any unintentional loading, as rabbits were allowed unrestricted cage activity postoperatively.

Backscattered electron imaging

After euthanasia, the distal femurs were trimmed with a band saw, and the soft tissue was dissected away. Femurs were fixed in 70% ethanol, dehydrated in ascending grades of ethanol to absolute, cleared in xylene, infiltrated, and embedded in methyl methacrylate.[32] Polymethyl-methacrylate-embedded undecalcified sections were examined under a scanning electron microscope using a backscattered electron (BSE) detector at 50 times magnification. The operating conditions of the scanning electron microscope were 20 mm working distance, 30 kV accelerating voltage, 200 μm aperture setting, 0.78 A filament current, and 100 nA emissions current. A 5×2 mm area encompassing the porous implant and an adjacent 5×2 mm area of periprosthetic bone just below the implant interface were imaged (Fig. 2). The specimens were ground three times, removing 2, 0.5, and 0.5 mm of material, which exposed a new level of bone at 2, 2.5, and 3 mm within the 5-mm-diameter implant. Each time, the specimens were ground, repolished, and imaged to yield three levels per femur. The images were analyzed for the area (mm^2) occupied by bone impaction or ingrowth into the porous implant and the area (mm^2) of periprosthetic bone using a semiautomated image analysis system (Image J, NIH, Bethesda, MD). The area fraction of bone ingrowth and area fraction of periprosthetic bone were also calculated as the area occupied by bone divided by the available void space, which included the area occupied by bone and marrow.

Fluorochrome analysis

Xylenol orange and calcein were administered 14 and 3 days before necropsy,[33] respectively, via intravenous injection in all experimental and time zero animals. In the case of the time zero animals, necropsy was performed directly after bilateral implantation surgery. After BSE image analysis, the polished surfaces of the sections were attached to plastic slides, and then ground and polished to a thickness of approximately 20–40 μm. The sections were viewed at a magnification of 200× under a mercury lamp microscope for evidence of fluorochrome double-labeled trabeculae in ingrown and periprosthetic bone. The regions of interest were the same as those used for BSE imaging. Five measurements were made along the span of each double label, and five double labels were measured for bone formation in the porous implant and periprosthetic bone for each section. Images were analyzed using a commercial histomorphometric system (Bioquant, Nashville, TN). The thickness of newly mineralized bone at the surface of the trabeculae was averaged along the length of the active bone-forming surface, divided by the 11-day labeling interval, and expressed as the MAR in units of microns per day.

Histological analysis

After fluorescence microscopy, the undecalcified sections were stained with a surface stain, Pico Sirius Red (Fisher Scientific, Fair Lawn, NJ). Sections were examined at ×25 to ×400 magnifications using transmitted light microscopy. After analysis, the sections were reground, polished, stained with Sanderson Rapid Bone Stain (Surgipath Medical Industries, Richmond, IL), and counterstained with Acid

Table 1. Backscattered Electron Imaging and Fluorescent Microscopy Results (Mean ± SD)

	Time zero	*Loaded*	*Control*
Bone ingrowth			
%	1 ± 1	21 ± 4	15 ± 5
mm^2	0.1 ± 0.1	1.8 ± 0.3	1.3 ± 0.4
Mineral apposition rate (μm/day)	No labels	2.6 ± 0.4	2.7 ± 0.6
Periprosthetic			
%	22 ± 3	29 ± 8	25 ± 9
mm^2	1.8 ± 0.3	2.9 ± 0.8	2.5 ± 0.8
Mineral apposition rate (μm/day)	1.8 ± 0.6	2.5 ± 0.6	2.2 ± 0.9

Bone ingrowth at time zero indicates bone that was impacted into the implant during surgery.

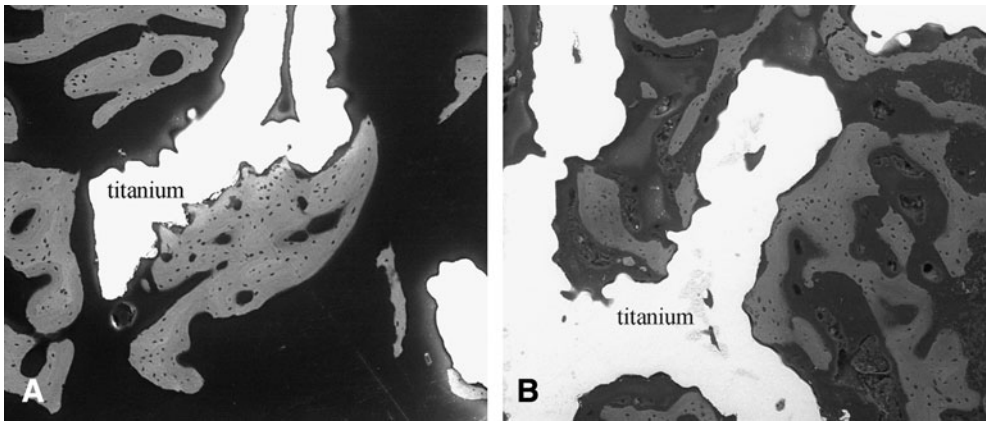

FIG. 3. Backscattered electron image at 200× demonstrating osseointegration (gray) within a porous titanium implant (white) in a control (**A**) and loaded (**B**) limb.

Fuschin (Fisher Scientific). Sections were again examined at ×25 to ×400 magnifications using both transmitted and polarized light microscopy. For both stains, the bone–implant interface was analyzed qualitatively for osseointegration, the formation of woven bone, and the formation of fibrous tissue. The host tissue response to the porous implant was also analyzed at the bone–implant interface.

Statistical analysis

Data were analyzed for the effect of *in vivo* loading on percent bone ingrowth, percent periprosthetic bone, and MAR of bone ingrowth and periprosthetic bone. A linear mixed effects model was used to account for repeated measures and the correlation of the outcome measures within rabbits. Analysis was performed using SAS software (9.1; SAS Institute Cary, NC), with significance set at $p < 0.05$. All data are presented as mean ± standard deviation.

Results

Baseline time zero specimens

BSE imaging of the time zero limbs confirmed that the porous implants were accurately placed under the core of the loading device, above a bed of viable cancellous periprosthetic host bone. The percent area of underlying cancellous periprosthetic bone beneath the implant was 22% ± 3% in the time zero specimens. Histological analysis demonstrated regions of hematoma around the periphery. BSE imaging and histological analysis both showed that the initial operation created a blunt boundary between the implant and periprosthetic host tissue, with no gap created at this interface, leaving bone in close apposition to the implant (Fig. 2). BSE imaging also demonstrated that minimal bone (1% ± 1%) was impacted into the porous implants during the operation. The MAR of the periprosthetic bone was (1.8 ± 0.6 μm/day) in the time zero rabbits.

Bone ingrowth

Two animals did not complete the 4-week experiment due to complications associated with patellar dislocation and were excluded from the study. BSE imaging was conducted on the remaining eight animals, and bone ingrowth was present in the porous implant of both the loaded and control limbs. However, the amount bone ingrowth was significantly greater in the loaded limb (21% ± 4%) compared to the control limb (15% ± 5%, $p = 0.03$) (Table 1). Bone was in direct apposition to the coatings in both loaded and nonloaded implants (Fig. 3). The presence of the initial fluorochrome

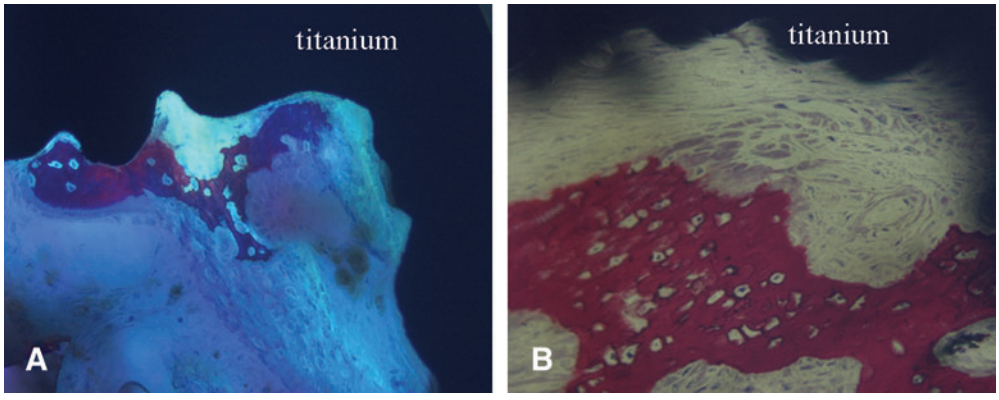

FIG. 4. Transmitted light microscopy images showing new woven bone (pink) near the porous titanium implant (black) in control (**A**) (200×) and loaded (**B**) (200×) limbs from the same rabbit. Unstained unmineralized osteoid can be observed (**A**) below the newly formed woven bone. Osteoblasts can be seen along the periphery of the newly formed woven bone (**B**). Color images available online at www.liebertonline.com/ten.

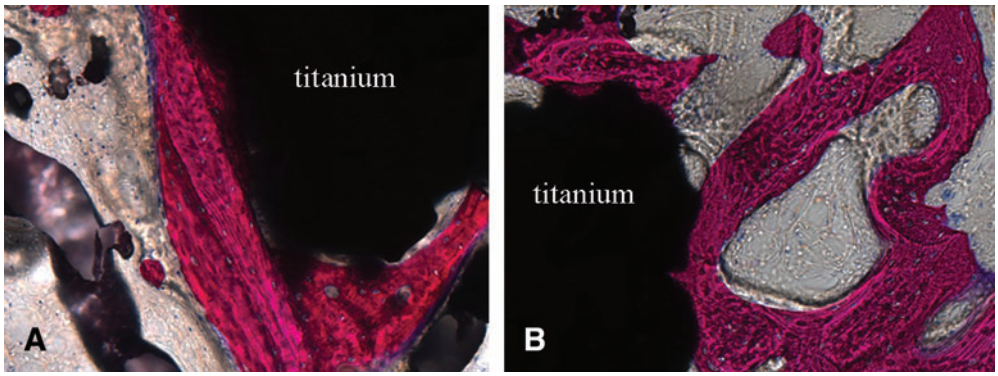

FIG. 5. Transmitted light microscopy images demonstrating direct bone apposition (pink) to the porous titanium implant (black) in control (**A**) (200×) and loaded (**B**) (200×) limbs from the same rabbit. Color images available online at www.liebertonline.com/ten.

label administered at day 14 and the second label administered at day 25 of loading confirmed that mineralized bone tissue was formed within the porous implant between these time points. MAR of the bone ingrowth was not different between the loaded ($2.6 \pm 0.4\,\mu m/day$) and control limbs ($2.7 \pm 0.6\,\mu m/day$, $p = 0.73$). The porous implant allowed bone ingrowth in all specimens with no adverse inflammatory response observed histologically.

Histological analysis demonstrated that the characteristics of osseointegration were similar between the loaded and nonloaded control implants in that newly formed woven bone was observed within the porous coated (Fig. 4) and periprosthetic regions of both the loaded and nonloaded limbs. Additionally, woven bone within the porous coated region was observed in direct apposition to the coatings of both the loaded and nonloaded limbs (Fig. 5). Remodeling activity was identified in bone tissue within the implant in all specimens. Using transmitted and polarized light microscopy, isolated areas of fibrous tissue were observed within the porous coating and were at times interposed between the coating and bone ingrowth in both loaded and nonloaded implants (Fig. 6). Active remodeling was observed at these sites, with osteoblasts present along the osteoid seam of the bone, adjacent to the fibrous tissue and coating surface. However, bone within the porous coating of both loaded and nonloaded implants was continuous with periprosthetic bone, with no specimens demonstrating fibrous tissue encapsulation at the periprosthetic bone–implant interface boundary layer.

Periprosthetic bone

The percent area of underlying cancellous periprosthetic bone beneath the implant was not different between the loaded ($29\% \pm 8\%$) and control limbs ($25\% \pm 9\%$, $p = 0.37$) (Fig. 2). The presence of fluorochrome labels administered at day 14 and 25 of loading confirmed periprosthetic host bone apposition at these time points. MAR of periprosthetic bone was also not different between the loaded ($2.5 \pm 0.6\,\mu m/day$) and control limbs ($2.2 \pm 0.9\,\mu m/day$, $p = 0.52$) (Table 1 and Fig. 6). The MAR and the percent area of the periprosthetic tissue was greater in the loaded limbs than in the baseline time zero controls. Histological characteristics of periprosthetic tissue were similar between the loaded and nonloaded control, with active sites of bone remodeling and sites of new woven bone observed in all specimens. Both woven bone and more mature lamellar periprosthetic bone were observed in direct apposition to the peripheral porous coating.

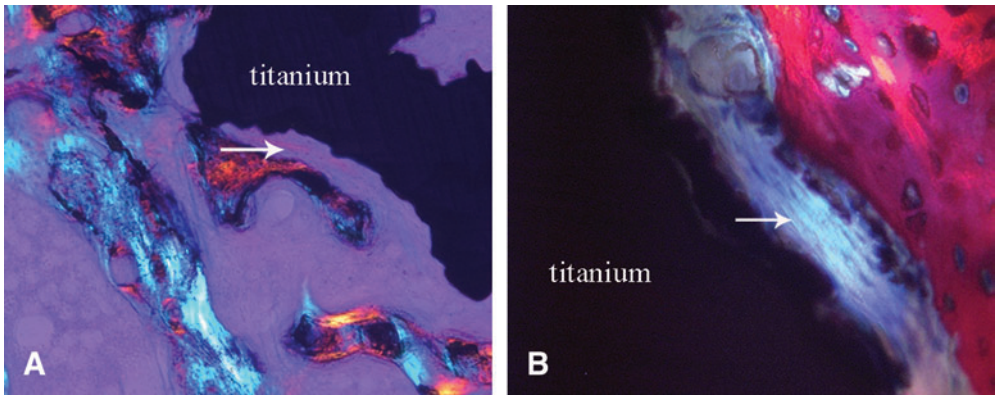

FIG. 6. Polarized (**A**) and transmitted (**B**) light microscopy images demonstrating fibrous tissue formation (arrows) interposed between bone ingrowth (pink) and a porous titanium implant (black) in control (**A**) (200×) and loaded (**B**) (400×) limbs from the same rabbit. Osteoblasts (dark blue) can be observed at the edge of newly formed woven bone (pink) adjacent to fibrous tissue (**B**). Color images available online at www.liebertonline.com/ten.

Discussion

The *in vivo* model presented in our study demonstrated that cyclic mechanical loading significantly enhanced bone ingrowth into the porous implants as shown through comparison of the loaded limbs and nonloaded controls. The amount of bone ingrowth measured in the loaded limb was at the high end of what has been reported in other studies examining bone ingrowth in the distal femur of rabbits after 4 weeks implantation.[14,30] The amount of bone ingrowth in this animal model was likely limited by the relatively small amount of cancellous host bone present in the rabbit distal femur, as has been demonstrated in the analysis of postmortem retrieved human total joint implants that the amount of host and periprosthetic tissue influences the amount of bone ingrowth.[34,35]

In the current study, the MAR of periprosthetic tissue in the time zero baseline controls was lower than either loaded or control limbs. Therefore, the presence of the porous implant and/or the implanted loading device may have led to a regional acceleratory phenomenon,[36] stimulating a local acceleration of bone remodeling in both the loaded and control limbs. The MAR of periprosthetic tissue in the current investigation was similar to that of a previous study by our group using the same implantable *in vivo* loading device applying a force directly to the surface of the cancellous host bone without the presence of a porous titanium foam implant.[18] The similarity of these results suggests that the implantation of the loading device alone was sufficient to cause this acceleration in MAR. Our fluorochrome labeling was conducted between 14 and 25 days of loading to minimize the contribution of this response, which is likely more pronounced immediately after surgery. However, it remains unclear if and at what time point the additional stimulus of loading may be reflected in the MAR measurements of ingrown bony tissue or periprosthetic tissue in this osseointegration model. In addition, during the initial weeks after surgical trauma, repair processes involving cytokines and pluripotent mesenchymal cells may cause an all-or-none reaction in bone MARs that is independent of any loading regime.[37]

The lack of fibrous tissue layer at the bone–implant interface demonstrates that the benefits of loading can be achieved without the detrimental effects of micromotion between the device and the surrounding tissues. These data are supported by investigations in dental[38] and orthopedic implants[39] that also observed that early loading can promote bone osseointegration without fibrous tissue formation at the bone–implant interface. A threshold of micromotion exists that affects bone healing and osseointegration, above which more fibrous tissue than bone forms,[26,40–43] leading to a layer of fibrous tissue at the bone–implant interface.[28] The threshold of micromotion, however, is likely influenced by the implant surfaces themselves. Previous experiments were mainly conducted with implants with smooth surfaces or older coating technologies (such as beaded surfaces) that may not have provided adequate friction between the implant and bone surfaces during the early stages of the healing process to minimize micromotion.

Surface design, including pore size,[44] directly influences early implant stability and healing, thereby affecting the potential for implant osseointegration. We utilized a novel titanium foam implant material that allowed cancellous bone ingrowth at the interface of the porous implant by a combination of bone appositional formation and intramembranous bone-healing processes. This porous coating has robust osteoconductive properties, resulting in a comparable bone ingrowth to that of conventional sintered beaded implants in a distal medial parapatellar arthrotomy rabbit model.[30]

Our study has limitations. We investigated osseointegration in a cylindrical implant; translating this study to a more complex geometry of a femoral component or tibial component will not be trivial given the more complex geometries and loading conditions. Also, we only investigated the remodeling response after 14 and 25 days of loading, which is inadequate to determine if the enhanced bone ingrowth will remain with longer times. Further investigations using more complex geometries and additional time points will be required to address these limitations. However, the *in vivo* loading model holds a great deal of potential to examine a host of clinical problems including how *in vivo* biophysical stimulation influences defect healing in cancellous bone using approaches involving nonmetallic cell seeded scaffolds.

Using this novel *in vivo* model, cancellous bone osseointegration into a porous titanium foam implant in the rabbit distal femur was enhanced in response to 4 weeks of applied controlled mechanical loading. This enhancement was achieved without the presence of a fibrous tissue layer at the bone–implant interface previously observed in other models that used older implant coating technologies. These findings are promising and provide a basis for future investigations that are required to understand the mechanism involved in the loading response and, eventually, whether long-term fixation may be enhanced clinically by appropriate exercise.

Acknowledgments

This study was partially supported by the Clark and Kirby Foundations and utilized the facilities of the Musculoskeletal Repair and Regeneration Core Center (NIH P30-AR046121). The porous titanium foam implants were kindly provided by Smith and Nephew, Inc.

Disclosure Statement

No competing financial interests exist.

References

1. Albrektsson, T., Branemark, I.-I., Hansson, H.-A., and Lindstrom, J. Osseointegrated titanium implants. Acta Orthop Scand **52,** 155, 1981.
2. Sumner, D.R., Kienapfel, H., Jacobs, J.J., Urban, R.M., Turner, T.M., and Galante, J.O. Bone ingrowth and wear debris in well-fixed cementless porous-coated tibial components removed from patients. J Arthroplasty **10,** 157, 1995.
3. Hofmann, A.A., Bloebaum, R.D., and Bachus, K.N. Progression of human bone ingrowth into porous-coated implants. Rate of bone ingrowth in humans. Acta Orthop Scand **68,** 161, 1997.
4. Whiteside, L.A. Long-term followup of the bone-ingrowth Ortholoc knee system without a metal-backed patella. Clin Orthop Relat Res **388,** 77, 2001.
5. Collier, J.P., Mayor, M.B., Chae, J.C., Surprenant, V.A., Surprenant, H.P., and Dauphinais, L.A. Macroscopic and

microscopic evidence of prosthetic fixation with porous-coated materials. Clin Orthop Relat Res **235,** 173, 1988.
6. Cook, S.D., Thomas, K.A., and Haddad, R.J., Jr. Histologic analysis of retrieved human porous-coated total joint components. Clin Orthop Relat Res **234,** 90, 1988.
7. Pidhorz, L.E., Urban, R.M., Jacobs, J.J., Sumner, D.R., and Galante, J.O. A quantitative study of bone and soft tissues in cementless porous-coated acetabular components retrieved at autopsy. J Arthroplasty **8,** 213, 1993.
8. Bobyn, J.D. Fixation and bearing surfaces for the next millennium. Orthopedics **22,** 810, 1999.
9. Galante, J. Total hip replacement. Orthop Clin North Am **2,** 139, 1971.
10. Jones, L.C., and Hungerford, D.S. Cement disease. Clin Orthop Relat Res **225,** 192, 1987.
11. Landon, G.C., Galante, J.O., and Maley, M.M. Noncemented total knee arthroplasty. Clin Orthop Relat Res **205,** 49, 1986.
12. Bobyn, J.D., Poggie, R.A., Krygier, J.J., Lewallen, D.G., Hanssen, A.D., Lewis, R.J., Unger, A.S., O'Keefe, T.J., Christie, M.J., Nasser. S., Wood, J.E., Stulberg, S.D., Tanzer, M. Clinical validation of a structural porous tantalum biomaterial for adult reconstruction. J Bone Joint Surg Am **86A Suppl 2,** 123, 2004.
13. Bobyn, J.D., Stackpool, G.J., Hacking, S.A., Tanzer, M., and Krygier, J.J. Characteristics of bone ingrowth and interface mechanics of a new porous tantalum biomaterial. J Bone Joint Surg Br **81,** 907, 1999.
14. Deglurkar, M., Davy, D.T., Stewart, M., Goldberg, V.M., and Welter, J.F. Evaluation of machining methods for trabecular metal implants in a rabbit intramedullary osseointegration model. J Biomed Mater Res B Appl Biomater **80,** 528, 2007.
15. Hulbert, S.F., Matthews, J.R., Klawitter, J.J., Sauer, B.W., and Leonard, R.B. Effect of stress on tissue ingrowth into porous aluminum oxide. J Biomed Mater Res **8,** 85, 1974.
16. Leucht, P., Kim, J.B., Wazen, R., Currey, J.A., Nanci, A., Brunski, J.B., and Helms, J.A. Effect of mechanical stimuli on skeletal regeneration around implants. Bone **40,** 919, 2007.
17. Rubin, C.T., and McLeod, K.J. Promotion of bony ingrowth by frequency-specific, low-amplitude mechanical strain. Clin Orthop Relat Res **298,** 165, 1994.
18. van der Meulen, M.C., Morgan, T.G., Yang, X., Baldini, T.H., Myers, E.R., Wright, T.M., and Bostrom, M.P. Cancellous bone adaptation to *in vivo* loading in a rabbit model. Bone **38,** 871, 2006.
19. Waldorff, E.I., Goldstein, S.A., and McCreadie, B.R. Age-dependent microdamage removal following mechanically induced microdamage in trabecular bone *in vivo*. Bone **40,** 425, 2007.
20. Duyck, J., Cooman, M.D., Puers, R., Van Oosterwyck, H., Sloten, J.V., and Naert I. A repeated sampling bone chamber methodology for the evaluation of tissue differentiation and bone adaptation around titanium implants under controlled mechanical conditions. J Biomech **37,** 1819, 2004.
21. Vandamme, K., Naert, I., Geris, L., Sloten, J.V., Puers, R., and Duyck, J. Histodynamics of bone tissue formation around immediately loaded cylindrical implants in the rabbit. Clin Oral Implants Res **18,** 471, 2007.
22. Duyck, J., Slaets, E., Sasaguri, K., Vandamme, K., and Naert, I. Effect of intermittent loading and surface roughness on peri-implant bone formation in a bone chamber model. J Clin Periodontol **34,** 998, 2007.
23. Geris, L., Vandamme, K., Naert, I., Vander Sloten, J., Duyck, J., and Van Oosterwyck, H. Application of mechanoregulatory models to simulate peri-implant tissue formation in an *in vivo* bone chamber. J Biomech **41,** 145, 2008.
24. Vandamme, K., Naert, I., Geris, L., Vander Sloten, J., Puers, R., and Duyck, J. Influence of controlled immediate loading and implant design on peri-implant bone formation. J Clin Periodontol **34,** 172, 2007.
25. Goodman, S., and Aspenberg, P. Effects of mechanical stimulation on the differentiation of hard tissues. Biomaterials **14,** 563, 1993.
26. Pilliar, R.M., Lee, J.M., and Maniatopoulos, C. Observations on the effect of movement on bone ingrowth into porous-surfaced implants. Clin Orthop Relat Res **208,** 108, 1986.
27. Soballe, K., Hansen, E.S., Rasmussen, H., Jorgensen, P.H., and Bunger, C. Tissue ingrowth into titanium and hydroxyapatite-coated implants during stable and unstable mechanical conditions. J Orthop Res **10,** 285, 1992.
28. Bragdon, C.R., Burke, D., Lowenstein, J.D., O'Connor, D.O., Ramamurti, B., Jasty, M., and Harris, W.H. Differences in stiffness of the interface between a cementless porous implant and cancellous bone *in vivo* in dogs due to varying amounts of implant motion. J Arthroplasty **11,** 945, 1996.
29. Soballe, K., Hansen, E.S., Brockstedt-Rasmussen, H., and Bunger, C. Hydroxyapatite coating converts fibrous tissue to bone around loaded implants. J Bone Joint Surg Br **75,** 270, 1993.
30. Willie, B., Yang, X., Kelly, N., Merkow, J., Ware, R., Gagne, S., Wright, T., and Bostrom, M. Osseointegration into a novel titanium foam implant in the distal femur of a rabbit. J Biomed Mater Res Part B **92,** 479, 2010.
31. van der Meulen, M.C., Yang, X., Morgan, T.G., and Bostrom, M.P. The effects of loading on cancellous bone in the rabbit. Clin Orthop Relat Res **467**, 2000, 2009.
32. Erben, R.G. Embedding of bone samples in methylmethacrylate: an improved method suitable for bone histomorphometry, histochemistry, and immunohistochemistry. J Histochem Cytochem **45,** 307, 1997.
33. van Gaalen, S.M., Kruyt, M.C., Geuze, R.E., de Bruijn, J.D., Alblas, J., and Dhert, W.J. Use of fluorochrome labels in *in vivo* bone tissue engineering research. Tissue Eng Part B Rev **16,** 209, 2010.
34. Bloebaum, R.D., Bachus, K.N., Jensen, J.W., Scott, D.F., and Hofmann, A.A. Porous-coated metal-backed patellar components in total knee replacement. A postmortem retrieval analysis. J Bone Joint Surg Am **80,** 518, 1998.
35. Bloebaum, R.D., Mihalopoulus, N.L., Jensen, J.W., and Dorr, L.D. Postmortem analysis of bone growth into porous-coated acetabular components. J Bone Joint Surg Am **79,** 1013, 1997.
36. Frost, H. Intermediary Organization of the Skeleton. Boca Raton, FL: CRC Press, 1986.
37. Lamerigts, N.M., Buma, P., Huiskes, R., Schreurs, W., Gardeniers, J., and Slooff, T.J. Incorporation of morsellized bone graft under controlled loading conditions. A new animal model in the goat. Biomaterials **21,** 741, 2000.
38. Meyer, U., Joos, U., Mythili, J., Stamm, T., Hohoff, A., Fillies, T., Stratmann, U., and Wiesmann, H.P. Ultrastructural characterization of the implant/bone interface of immediately loaded dental implants. Biomaterials **25,** 1959, 2004.
39. Rostlund, T., Carlsson, L., Albrektsson, B., and Albrektsson, T. Osseointegrated knee prostheses. An experimental study in rabbits. Scand J Plast Reconstr Surg Hand Surg **23,** 43, 1989.
40. Ducheyne, P., De Meester, P., and Aernoudt, E. Influence of a functional dynamic loading on bone ingrowth into surface pores of orthopedic implants. J Biomed Mater Res **11,** 811, 1977.

41. Cameron, H.U., Pilliar, R.M., and MacNab, I. The effect of movement on the bonding of porous metal to bone. J Biomed Mater Res **7,** 301, 1973.
42. Uhthoff, H.K. Mechanical factors influencing the holding power of screws in compact bone. J Bone Joint Surg Br **55,** 633, 1973.
43. Simmons, C.A., Valiquette, N., and Pilliar, R.M. Osseointegration of sintered porous-surfaced and plasma spray-coated implants: an animal model study of early postimplantation healing response and mechanical stability. J Biomed Mater Res **47,** 127, 1999.
44. Bobyn, J.D., Pilliar, R.M., Cameron, H.U., and Weatherly, G.C. The optimum pore size for the fixation of porous-surfaced metal implants by the ingrowth of bone. Clin Orthop Relat Res **150,** 263, 1980.

Address correspondence to:
Bettina M. Willie, Ph.D.
Julius Wolff Institut
Charité-Universitätsmedizin Berlin
Campus Virchow-Klinkum
Forum 4, Postfach 24
Augustenburger Platz 1
Berlin 13353
Germany

E-mail: bettina.willie@charite.de

Received: December 3, 2009
Accepted: April 1, 2010
Online Publication Date: May 17, 2010